How to Cite:
Bhosale, M. S., & Saravanan, K. (2022). Comparative synthetic study, in silico screening and biological evaluation of some substituted tetrahydropyrimidine-2-one derivatives as potential DHFR inhibitors. *International Journal of Health Sciences*, *6*(S3), 2814–2834. https://doi.org/10.53730/ijhs.v6nS3.6198

Comparative synthetic study, in *silico* screening and biological evaluation of some substituted tetrahydropyrimidine-2-one derivatives as potential DHFR inhibitors

M. S. Bhosale
Department of Pharmaceutical Chemistry, Bhagwant University, Ajmer

K. Saravanan
Department of Pharmaceutical Chemistry, Bhagwant University, Ajmer

***Abstract*---**In present study we have selected pyrimidine scaffold to design and develop some DHFR inhibitors as potential antibacterial and antifungal agents. The designed derivatives were first screened through ADMET property calculations and then those possess drug-likeness properties were subjected for the molecular docking studies. The derivatives which were found to be significant DHFR inhibition potential were subjected for the synthesis followed by spectral analysis and biological evaluation. From this virtual screening, it was concluded that all the compounds possess drug-like properties and hence were subjected to molecular docking studies. The selected derivatives were synthesized and subjected for in vitro biological evaluation. The comparative study for synthesis of the derivatives such as conventional, ultrasonic, microwave synthesis was carried out. It was also observed that yield of the compound was very good in microwave assisted synthesis i.e. 73.24% which is almost 30-40% more than that of the conventional and ultrasonic method. In mass spectrum it was observed that, product obtained through microwave method was completely pure and did not displayed any peak of starting material, whereas product obtained through conventional and ultrasonic method showed presence of starting material. Therefore we concluded that the microwave assisted synthesis method is most suitable for the synthesis of tetrahydropyrimidine-2-one derivatives through Biginelli reaction. We hereby report that, all the compounds A1, A2, A3, A4, A5, A6, A7, and A8 were found to be are potent and can be developed further to get more promising molecules for the treatment of bacterial & fungal infections.

International Journal of Health Sciences ISSN 2550-6978 E-ISSN 2550-696X © 2022.
***Corresponding author**: Bhosale, M. S.; Email: mayurbhosale2399@gmail.com*
Manuscript submitted: 18 Dec 2021, Manuscript revised: 27 March 2022, Accepted for publication: 09 April 2022

***Keywords*---**DHFR, tetrahydropyrimidine, Biginelli reaction, antibacterial activity, microwave.

Introduction

Inhibitors of dihydrofolate reductase (DHFR), an essential enzyme in the folate biosynthetic pathway, have been pursued for several decades as therapeutics in the treatment of human malignancies. DHFR catalyzes the transfer of a hydride from the cofactor, nicotinamide adenine dinucleotide phosphate (NADPH), to the substrate, dihydrofolate, thus yielding tetrahydrofolate and NADP+. Tetrahydrofolate is an essential cofactor in the production of purines and thymidylate and its deficiency leads to the inhibition of cell growth and proliferation(Nepali et al., 2014; Shahi & Kumar, 2016; Todd & Gomez, 2001; Wróbel et al., 2020).

One of the most serious risks to public health today is the emergence of germs that are resistant to the majority of the common treatment medications(Murali et al., 2014; Sánchez-Sánchez et al., 2017). Drug-resistant bacteria, such as methicillin-resistant *Staphylococcus aureus* (MRSA) and multidrug-resistant *Escherichia coli*, cause great difficulties in the treatment of nosocomial infections, which severely threaten global public health(Anwar et al., 2020; Jouhar et al., 2020; Loi et al., 2019). According to a UK Government analysis, "the cost in terms of lost global productivity between now and 2050 will be an astonishing 100 trillion USD if we do not take action". Fungal infections can represent a major hazard to human health, particularly in immunocompromised people.

Compounds based on the pyrimidine scaffold are known to exhibit many different biological actions such as antibacterial, antifungal, anti-inflammatory and antitumor activities(Mittersteiner et al., 2021; Nerkar, 2021; Verma et al., 2020). Lots of amino pyrimidine-based derivatives have been reported to exhibit antibacterial activities via inhibiting DHFR(Ahmed Elkanzi, 2020; Bhat et al., 2017). Therefore, in present study we have selected pyrimidine scaffold to design and develop some DHFR inhibitors as potential antibacterial and antifungal agents. The designed derivatives were first screened through ADMET property calculations and then those possess drug-likeness properties were subjected for molecular docking studies. The derivatives which were found to be significant DHFR inhibition potential were subjected for synthesis followed spectral analysis and biological evaluation. The comparative study for synthesis of the derivatives such as conventional, ultrasonic, and microwave synthesis was carried out. The one compound synthesized from each method were studied to prove the most effective method.

Materials and methods

Pharmacokinetics and toxicity predictions of designed derivatives

Utilizing molinspiration and SwissADME servers, Lipinski rule of five and pharmacokinetic features of developed derivatives were investigated(Daina et al., 2017; Kim et al., 2021). An *in silico* toxicity prediction of designed derivatives has

been made using ProTox-II, a webserver that is freely available (http://tox.charite.de/protox_II)(Banerjee et al., 2018).

Molecular Docking

After screening through *in silico* ADMET analysis, the screened molecules were subjected for the molecular docking studies. The proposed derivatives and the native ligand were docked against the crystal structure of the wild-type *E. coli* dihydrofolate reductase using Autodock vina 1.1.2 in PyRx 0.8(Dallakyan & Olson, 2015). ChemDraw Ultra 8.0 was used to draw the structures of the intended derivatives and native ligand (mole. File format). All the ligands were subjected for energy minimization by applying Universal Force Field (UFF)(Rappé et al., 1992). RCSB Protein Data Bank (PDB) entry 5CCC contains the wild-type *E. coli* dihydrofolate reductase complexed with 5, 10-dideazatetrahydrofolate and oxidized nicotinamide adenine dinucleotide phosphate (https://www.rcsb.org/structure/5CCC). Discovery Studio Visualizer (version-19.1.0.18287) was used to refine the enzyme structure, purify it, and get it ready for docking(San Diego: Accelrys Software Inc., 2012). A three-dimensional grid box (size_x= 30.6812046484Å; size_y= 32.6755842638Å; size_z= 35.0196745629Å) with an exhaustiveness value of 8 was created for molecular docking(Dallakyan & Olson, 2015). BIOVIA Discovery Studio Visualizer was used to locate the protein's active amino acid residues. The approach outlined by Khan et al. was used to perform the entire molecular docking procedure, identify cavity and active amino acid residues(Chaudhari et al., 2020; S.L. Khan et al., 2020; Sharuk L. Khan et al., 2020, 2021; Siddiqui et al., 2021). Fig. 1 shows the revealed cavity of DHFR with the co-crystallize ligand molecule.

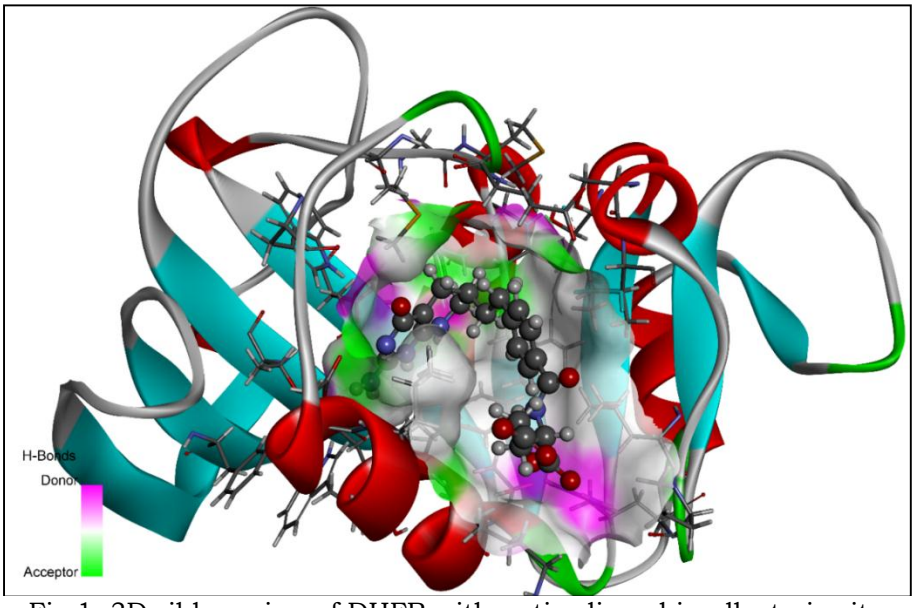

Fig 1. 3D ribbon view of DHFR with native ligand in allosteric site

Reaction scheme and synthesis of derivatives

All the required chemicals i.e. ethyl acetoacetate, aldehyde, urea, ferric chloride ($FeCl_3.6H_2O$), conc. HCl, ethanol, potassium hydroxide (KOH), and acetone of synthetic grade were purchased and procured from Lab Trading Laboratory, Aurangabad, Maharashtra, India. The progress of the reaction was confirmed by Thin-layer chromatography [TLC, (Merck precoated silica GF 254)] and compounds were subjected for spectral analysis by ^1H, ^{13}C NMR (on a Varian-VXR-300S at 400 MHz NMR spectrometer) and Mass spectroscopy with chloroform (d_6) as the solvent and TMS as the internal standard; chemical shift values were expressed in δ ppm. The melting points were measured using the VEEGO MODEL VMP-D melting point apparatus. The detailed procedure for the synthesis of derivatives is discussed in the below section.

Synthesis of 1, 2, 3, 4-tetrahydropyrimidine derivatives
Conventional synthesis

The reaction is a modified Biginelli reaction that generates 1, 2, 3, 4-tetrahydropyrimidine-2- *one* from ethyl acetoacetate, aldehyde and urea. A solution of ethyl acetoacetate (1.3gm, 10 mmol), urea (1.14gm, 15 mmol), ferric chloride ($FeCl_3.6H_2O$, 2.5 mmol) and conc. HCl (1-2 drops) in EtOH (20 mL) was heated independently with appropriate aldehydes (10 mmol), under reflux for 4-5 hrs[5]. After cooling, the reaction mixtures were poured onto crushed ice (100gm). Stirring was continued for several minutes, the solid products were filtered, independently washed with cold H_2O (2 times 50 mL) and a mixture of EtOH-H_2O, 1:1 (3 times 20 mL). The solids were dried and recrystallized from hot EtOH to afford pure products. The melting point was recorded. The yields obtained were in the range of 75-95%.

Ultrasonic synthesis

The mixture of 0.01 mole of urea, substituted aromatic aldehydes (0.01 mole) and ethyl acetoacetate (0.01 mole) is added into a beaker containing 10 ml of ethanol and subjected for ultra-sonication in an ultra sonicator at 220 Hz for requisite time until the completion of reaction. Checked by TLC. Filtered and recrystallized to offer title compounds.

Microwave synthesis

The mixture of 0.01 mole of urea, substituted aromatic aldehydes (0.01 mol) and ethyl acetoacetate (0.01 mol) is added into a RBF containing 10 ml of ethanol and subjected for Micro wave irradiation at 160W in a microwave reactor for requisite time until the completion of reaction was checked by TLC. The product formed was filtered and recrystallized to offer title compounds. The proposed reaction scheme for the synthesis of 1, 2, 3, 4-tetrahydropyrimidine derivatives is depicted in Fig 2 and the structures of the synthesized compounds are tabulated in Table 1 along with physicochemical parameters of synthesized compounds depicted in Table 2. The table 3 indicates the comparative data for the three methods of synthesis of tetrahydropyrimidine-2-one compound.

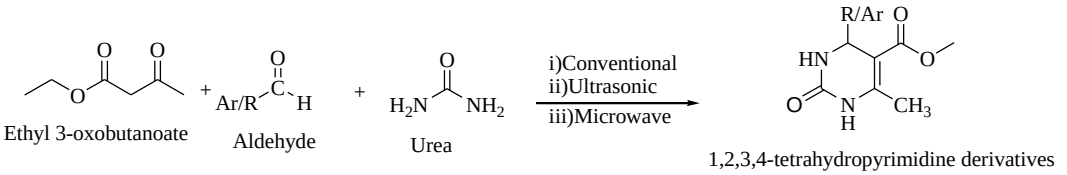

Fig 2. The proposed reaction scheme for the synthesis of 1, 2, 3, 4-tetrahydropyrimidine derivatives

Table 1
Structures of the synthesized compounds

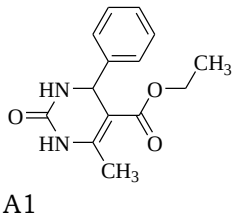 A1	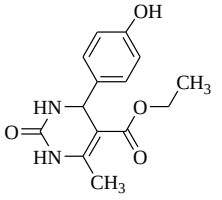 A2	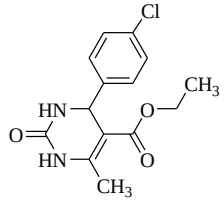 A3	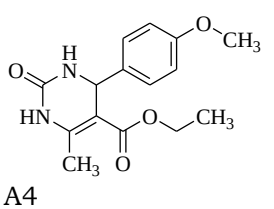 A4
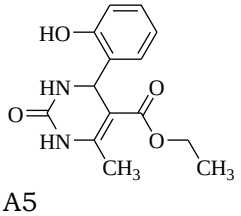 A5	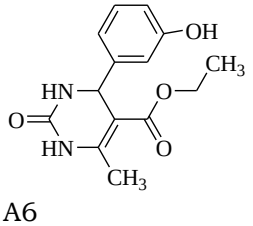 A6	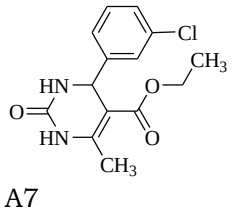 A7	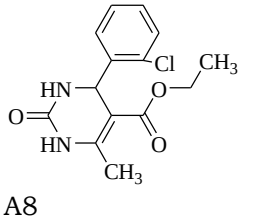 A8

Table 2
Physicochemical parameters of synthesized compounds

Comp.	Mol. Formula	Appearance	M.P.(^{0}C)	Rf value	Elemental Analyses calculated			
					C	H	N	O
A1	$C_{14}H_{16}N_2O_3$	Yellow	150-156	0.52	64.60	6.20	10.76	18.44
A2	$C_{14}H_{16}N_2O_4$	Slightly Yellow	156-162	0.78	60.86	5.84	10.14	23.16
A3	$C_{14}H_{15}ClN_2O_3$	Yellow	169-173	0.61	57.05	5.13	9.50	16.29
A4	$C_{15}H_{18}N_2O_4$	Pale Yellow	164-168	0.62	62.06	6.25	9.65	22.04
A5	$C_{14}H_{16}N_2O_4$	Brownish yellow	160-165	0.63	60.86	5.84	10.14	23.16
A6	$C_{14}H_{16}N_2O_4$	Yellow	140-146	0.78	60.86	5.84	10.14	23.16
A7	$C_{14}H_{15}ClN_2O_3$	Bright yellow	160-164	0.73	57.05	5.13	9.50	16.29
A8	$C_{14}H_{15}ClN_2O_3$	Yellow	163-167	0.84	57.05	5.13	9.50	16.29

Table 3
Comparative data for the three methods of synthesis of tetrahydropyrimidine-2-one compound

Comp	Time required for synthesis (Min.)			Percent practical yield		
	Conventional	Ultrasonic	Microwave	Conventional	Ultrasonic	Microwave
A1	89	32	2	63.25	56.25	73.25

A2	93	43	5	55.60	67.66	76.64
A3	107	35	2	53.34	56.23	73.24
A4	84	30	3	60.43	68.65	80.67
A5	94	38	5	53.34	61.86	75.87
A6	99	38	3	54.31	48.64	71.65
A7	99	39	2	52.21	52.78	72.79
A8	95	35	2	52.43	56.50	71.65

Spectral interpretation of synthesized compounds (microwave method)

A1. [*ethyl 6-methyl-2-oxo-4-phenyl-1,2,3,4-tetrahydropyrimidine-5-carboxylate*]

Molecular weight: 260.29 gm/mol. ^{1}H NMR ($CHCl_3$-*d6* 400 MHz) δ ppm: 1.4 (t, -CH_3 of acetate), □ 1.72 (s, -CH_3), □ 4.20 (d, -CH_2 of methyl), □ 6.56 (s, -methine), □ 6.5 (s, -NH of urea), □ 7.04, 7.04, 7.31, 7.31, 7.16 (m-Ar). ^{13}C NMR ($CHCl_3$-*d6* 400 MHz) δ ppm: 14.60, 15.00, 50.08, 108.34, 131.89, 138.83, 139.45, 145.45, 150.33, MS: m/z 261.30, 262.89 (m+1), 263.48 (m+2).

A2. [*ethyl 4-(4-hydroxyphenyl)-6-methyl-2-oxo-1,2,3,4-tetrahydropyrimidine-5-carboxylate*]

Molecular weight: 276.29 gm/mol. ^{1}H NMR ($CHCl_3$-*d6* 400 MHz) δ ppm: 1.50(t, -CH_3 of Acetate), □1.72 (s, -CH_3), □4.15 (d, -CH_2 of methyl), □ 5.60 (s, -methine), □6.50 (s, -NH of urea), □ 6.97, 6.58, 6.75, 6.89(q-Ar). ^{13}C NMR ($CHCl_3$-*d6* 400 MHz) δ ppm: 14.70, 15.20, 49.08, 67.98, 108.34, 116.23, 131.89, 138.83, 149.45, 168.33. MS: m/z 277.12, 278.14 (m+1), 279.28 (m+2).

A3. [*ethyl 4-(4-chlorophenyl)-6-methyl-2-oxo-1,2,3,4-tetrahydropyrimidine-5-carboxylate*]

Molecular weight: 294.63 gm/mol. ^{1}H NMR ($CHCl_3$-*d6* 400 MHz) δ ppm: 1.20(t, -CH_3 of Acetate), □1.78 (s, -CH_3), □ 4.25 (d, -CH_2 of methyl), □ 5.63 (s, -methine), □ 6.50 (s, -NH of urea), □ 7.45, 7.30, 7.15, 7.24(q, Ar). ^{13}C NMR ($CHCl_3$-*d6* 400 MHz) δ ppm: 14.10, 14.30, 49.08, 63.98, 108.34, 131.89, 138.83, 149.45, 168.33. MS: m/z 295.09, 296.17 (m+1), 297.08 (m+2).

A4. [*ethyl 4-(4-methoxyphenyl)-6-methyl-2-oxo-1,2,3,4-tetrahydropyrimidine-5-carboxylate*]

Molecular weight: 293.23 gm/mol. ^{1}H NMR ($CHCl_3$-*d6* 400 MHz) δ ppm: 1.10 (t, -CH_3 of Acetate), □ 1.72(s, -CH_3), □ 4.16 (d, -CH_2 of methyl), □ 5.45 (s, -methine), □ 6.03 (s, -NH of urea), □ 6.90, 6.34, 6.67, 6.34(q, Ar). ^{13}C NMR ($CHCl_3$-*d6* 400 MHz) δ ppm: 14.30, 15.0, 47.08, 54.98, 63.65, 105.37, 112.23, 129.08, 131.89, 137.76, 144.83, 152.45, 168.33. MS: m/z 291.89, 292.12(m+1), 293.34 (m+2).

In vitro biological evaluation

Various concentrations of derivatives were prepared in DMSO to assess their antibacterial and antifungal activities against standard strains using broth dilution. Bacteria were maintained, and drugs were diluted in nutrient Mueller Hinton broth. The broth was inoculated with 10^8 colony-forming units (cfu) per milliliter of test strains (Institute of Microbial Technology, Chandigarh, India) determined by turbidity. Stock solutions of synthesized derivate (2 mg/mL) were serially diluted for primary and secondary screening. The primary screen included 1000, 500, and 250 µg/mL of synthesized derivatives, then those with activity were further screened at 200, 100, 50, 25, 12.5, and 6.250 µg/mL. A control without antibiotic was sub-cultured (before inoculation) by spreading one loopful evenly over a quarter of a plate of medium suitable for growing test organisms and incubated at 37 ^{0}C overnight. The lowest concentrations of derivatives that inhibited bacterial or fungal growth were taken as minimal inhibitory concentrations (MICs). These were compared with the amount of control growth before incubation (original inoculum) to determine MIC accuracy. The standards for antibacterial activity were gentamycin, ampicillin, chloramphenicol, ciprofloxacin, and norfloxacin served, and those for antifungal activity were nystatin and griseofulvin. The antimalarial behavior was tested using plasmodium falciparum, with quinine and chloroquine as the standards(S. Khan et al., 2021; Shntaif et al., 2021). Both experiments took place at the Microcare laboratory and Tuberculosis Research Centre [TRC] in Surat, Gujarat.

Results

Pharmacokinetic characteristics are critical to drug development because they enable scientists to investigate the biological impacts of possible pharmacological candidates(A. Khan et al., 2022). This compound's oral bioavailability was evaluated using Lipinski's rule of five and Veber's rules (Table 4). To better understand the pharmacokinetics profiles and drug-likeness properties of the proposed compounds, the ADME characteristics of all of them were examined (Table 5). Fig. 3 depicts the physicochemical domain that is ideal for oral bioavailability. The oral acute toxicity have been predicted along with LD_{50} (mg/kg), toxicity class, hepatotoxicity, carcinogenicity, immunotoxicity, mutagenicity, and cytotoxicity (Table 6). Table 7 lists the ligand energies (kcal/mol), docking scores (kcal/mol), active amino acids, bond length (Å), and different interactions of derivatives with DHFR. Table 8 depicts the most potent compounds' 2D and 3D docking orientations. The results of antimicrobial and antifungal activities of the synthesized derivatives are tabulated in Table 9 which shows the MICs and MFCs respectively.

Table 4
Lipinski rule of 5 and Veber's rule calculated for molecules

Compound	Lipinski rule of five					Veber's rule	
	Log P	Mol. Wt.	HBA	HBD	Violations	Total polar surface area (Å^2)	No. of rotatable bonds
NL	0.70	443.45	7	6	2	187.50	10

A1	1.49	260.29	3	2	0	67.43	4
A2	0.95	276.29	4	3	0	87.66	4
A3	2.01	294.73	3	2	0	67.43	4
A4	1.2	290.31	4	2	0	76.66	5
A5	0.95	276.29	4	3	0	87.66	4
A6	0.95	276.29	4	3	0	87.66	4
A7	2.01	294.73	3	2	0	67.43	4
A8	2.01	294.73	3	2	0	67.43	4

Where: Mol. Wt., molecular weight; HBA, hydrogen bond acceptors; HBD, hydrogen bond donors

Table 5
The pharmacokinetics and drug-likeness properties of developed compounds

Comp codes	Pharmacokinetics									Drug-likeness			
	GI abs.	BBB pen.	P-gp sub.	CYP 1A2 inhibitors	CYP2 C19	CYP 2C9	CYP 2D6	CYP 3A4	Log K_p (skin permeation, cm/s)	Ghose	Egan	Muegge	Bioavailability Score
NL	Low	No	Yes	No	No	No	No	No	-8.81	0	1	2	0.11
A1	High	No	No	No	No	No	No	No	-6.91	0	0	0	0.55
A2	High	No	No	No	No	No	No	No	-7.26	0	0	0	0.55
A3	High	Yes	No	No	Yes	No	No	No	-6.67	0	0	0	0.55
A4	High	No	No	No	No	No	No	No	-7.11	0	0	0	0.55
A5	High	No	No	No	No	No	No	No	-7.26	0	0	0	0.55
A6	High	No	No	No	No	No	No	No	-7.26	0	0	0	0.55
A7	High	Yes	No	No	Yes	No	No	No	-6.67	0	0	0	0.55
A8	High	Yes	No	No	Yes	No	No	No	-6.67	0	0	0	0.55

Where: NL, Native ligand; GI abs., gastrointestinal absorption; BBB pen., blood brain barrier penetration; P-gp sub., p-glycoprotein substrate

Table 6
The predicted acute toxicity of molecules

Compd. codes	Parameters							
	LD_{50} (mg/kg)	Tox class	Prediction accuracy (%)	Hepatotoxicity (Probability)	Carcinogenicity	Immunotoxicity	Mutagenicity	Cytotoxicity
NL	135	3	67.38	I (0.87)	I (0.51)	I (0.99)	I (0.75)	I (0.63)
A1	2495	5	67.38	I (0.60)	A(0.56)	I (0.99)	I (0.65)	I (0.76)
A2	2495	5	54.26	I (0.56)	A(0.50)	I (0.99)	I (0.72)	I (0.84)
A3	1644	4	54.26	I (0.63)	A(0.53)	I (0.99)	I (0.67)	I (0.76)
A4	1644	4	54.26	I (0.59)	I (0.51)	I (0.98)	I (0.68)	I (0.89)
A5	3000	5	54.26	I (0.56)	I (0.50)	I (0.98)	I (0.72)	I (0.88)
A6	2495	5	54.26	I (0.56)	A(0.50)	I (0.98)	I (0.72)	I (0.84)
A7	1644	4	54.26	I (0.63)	A(0.53)	I (0.99)	I (0.67)	I (0.76)
A8	630	3	54.26	I (0.65)	A(0.51)	I (0.99)	I (0.68)	I (0.77)

Where: I, Inactive; A, Active

Table 7
The ligand energies (kcal/mol), docking scores (kcal/mol), active amino acids, bond length (Å), and different interactions of derivatives with DHFR

Active Amino Acid	Bond Length	Bond Type	Bond Category	Ligand Energy	Binding Affinity
A1					
TYR100	2.4769	Hydrogen Bond	Conventional Hydrogen Bond	243.79	-7.6
	3.97784	Hydrophobic	Pi-Sigma		
PHE31	3.62464				
MET20	4.47534	Other	Pi-Sulfur		
PHE31	4.9776	Hydrophobic	Pi-Pi T-shaped		
ILE5	5.45278		Pi-Alkyl		
ALA7	4.08883				
A2					
GLY15	2.9565	Hydrogen Bond	Conventional Hydrogen Bond	198.63	-7.9
TYR100	2.61842				
PHE31	3.61198	Hydrophobic	Pi-Sigma		
MET20	4.42626	Other	Pi-Sulfur		
PHE31	4.93917	Hydrophobic	Pi-Pi T-shaped		
ALA7	4.11353		Pi-Alkyl		
A3					
TYR100	2.19112	Hydrogen Bond	Conventional Hydrogen Bond	252.63	-8
GLY95	3.69884		Carbon Hydrogen Bond		
GLY96	3.45781				
	3.80026	Hydrophobic	Pi-Sigma		
PHE31	3.65811				
MET20	5.84595	Other	Pi-Sulfur		
ILE5	4.27268	Hydrophobic	Alkyl		
ALA7	4.13982		Pi-Alkyl		
TRP30	4.6451				
PHE31	5.19106				
A4					
TYR100	2.19112	Hydrogen Bond	Conventional Hydrogen Bond	224.79	-7.9
GLY95	3.69884		Carbon Hydrogen Bond		
GLY96	3.45781				
	3.80026	Hydrophobic	Pi-Sigma		
PHE31	3.65811				
MET20	5.84595	Other	Pi-Sulfur		
ILE5	4.27268	Hydrophobic	Alkyl		
ALA7	4.13982		Pi-Alkyl		
TRP30	4.6451				
PHE31	5.19106				
A5					
TYR100	2.54631	Hydrogen Bond		255.21	-7.8

ILE5	2.27392				
GLY96	3.67939		Carbon Hydrogen Bond		
	3.84445	Hydrophobic	Pi-Sigma		
PHE31	3.73316				
MET20	4.47393	Other	Pi-Sulfur		
ALA6,ALA7	4.09848	Hydrophobic	Amide-Pi Stacked		
ILE5	5.33884		Pi-Alkyl		
ALA7	4.18225				
A6					
TYR100	2.79001	Hydrogen Bond	Conventional Hydrogen Bond	243.7	-7.7
ASP27	1.82407				
PHE31	3.73003	Hydrophobic	Pi-Sigma		
MET20	4.37176	Other	Pi-Sulfur		
PHE31	4.82287	Hydrophobic	Pi-Pi T-shaped		
ALA7	4.20773		Pi-Alkyl		
A7					
PHE31	4.83589	Hydrophobic	Pi-Pi T-shaped	240.17	-7.8
ILE5	4.53235		Alkyl		
ALA6	5.09267		Pi-Alkyl		
ALA7	5.33453				
	4.37408				
TRP30	5.17032				
PHE31	4.96141				
A8					
GLY15	2.30393	Hydrogen Bond	Conventional Hydrogen Bond	277.67	-7.5
	2.87026				
PHE31	3.65121	Hydrophobic	Pi-Sigma		
MET20	3.9669				
	4.12137	Other	Pi-Sulfur		
PHE31	4.71105	Hydrophobic	Pi-Pi T-shaped		
ALA7	5.25308		Pi-Alkyl		
ILE5	5.41444				
ALA7	4.15187				
NL					
ASP27	1.89071	Hydrogen Bond	Conventional Hydrogen Bond	293.4	-8.6
	2.23099				
ILE5	2.04556				
	2.00364				
ARG57	2.14074				
	2.64414				
ILE94	3.10227		Carbon Hydrogen Bond		
PHE31	4.39543	Electrostatic	Pi-Cation		
ALA7	3.87526	Hydrophobic	Pi-Sigma		
ILE50	3.63978				
	5.85001		Pi-Pi T-shaped		
PHE31	4.96722				

	4.99602				
ILE5	5.33172		Pi-Alkyl		

Table 8
The 2D- and 3D binding orientations of native ligand and molecules selected for the synthesis from virtual screening

2D-binding orientations	3D-binding orientations
Native ligand	
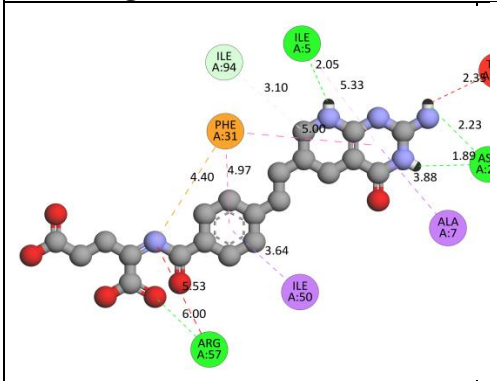	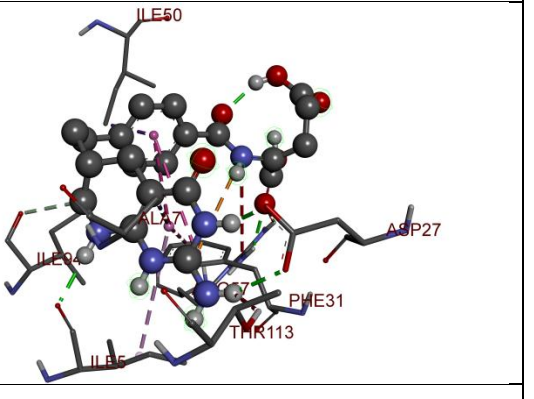
A1	
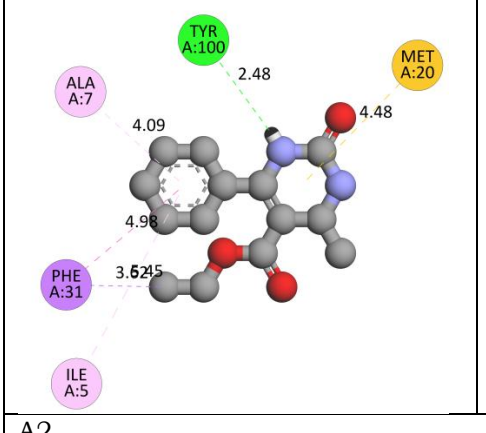	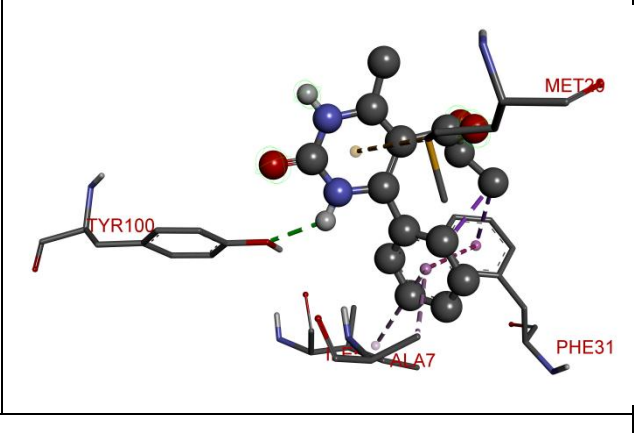
A2	
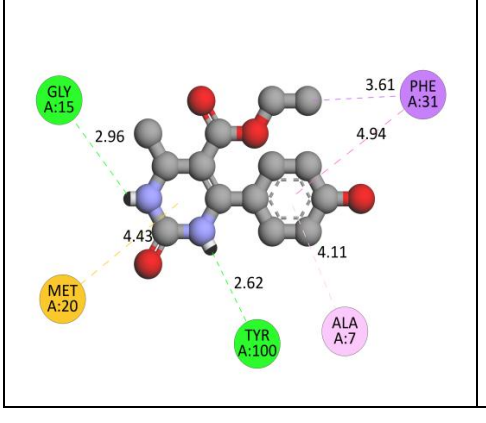	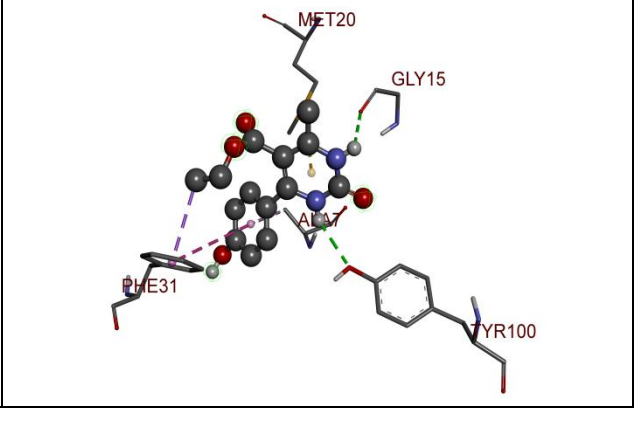

A3

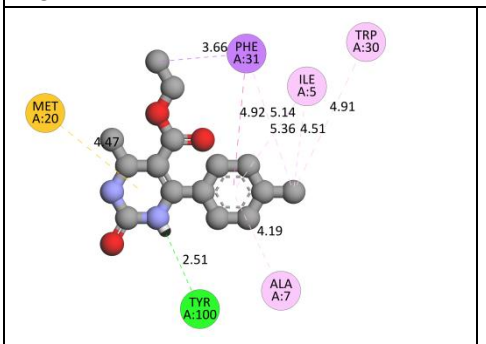
3.66
PHE A:31
TRP A:30
ILE A:5
MET A:20
4.92 5.14
4.91
5.36 4.51
4.47
4.19
2.51
ALA A:7
TYR A:100

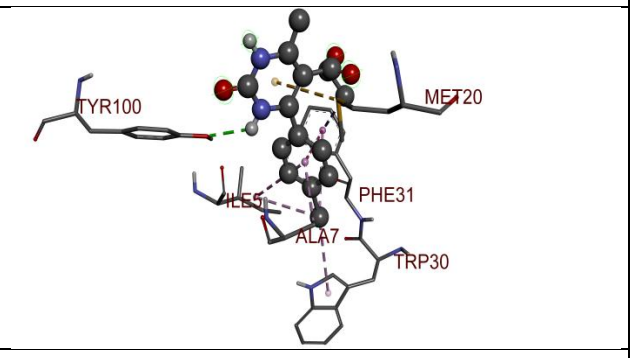
TYR100
MET20
PHE31
ILE5
ALA7
TRP30

A4

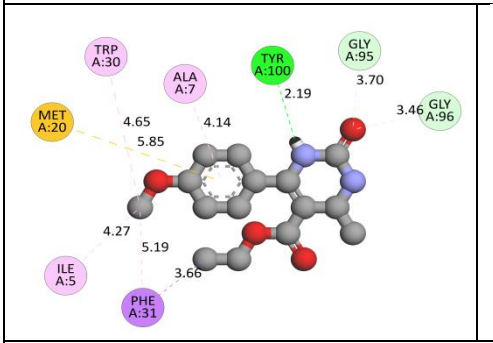
TRP A:30
ALA A:7
TYR A:100
GLY A:95
3.70
2.19
3.46
GLY A:96
MET A:20
4.65
4.14
5.85
4.27
5.19
3.66
ILE A:5
PHE A:31

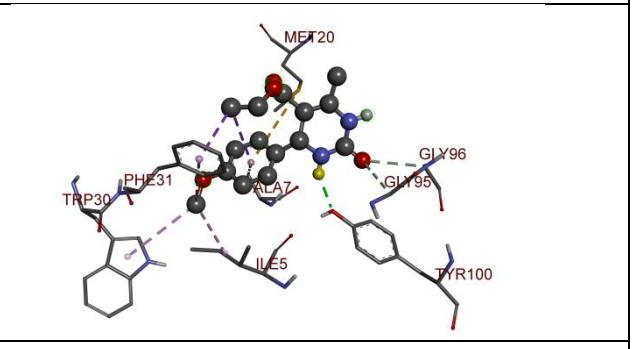
MET20
GLY96
PHE31
ALA7
GLY95
TRP30
ILE5
TYR100

A5

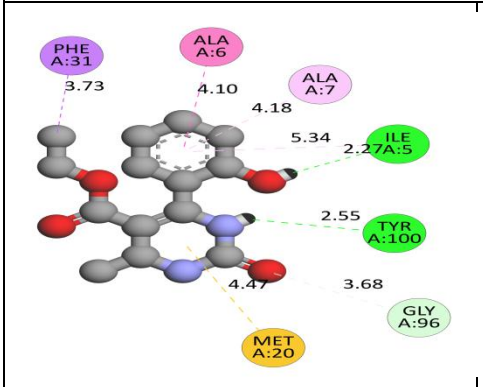
PHE A:31
ALA A:6
ALA A:7
3.73
4.10
4.18
5.34
ILE 2.27A:5
2.55
TYR A:100
4.47
3.68
GLY A:96
MET A:20

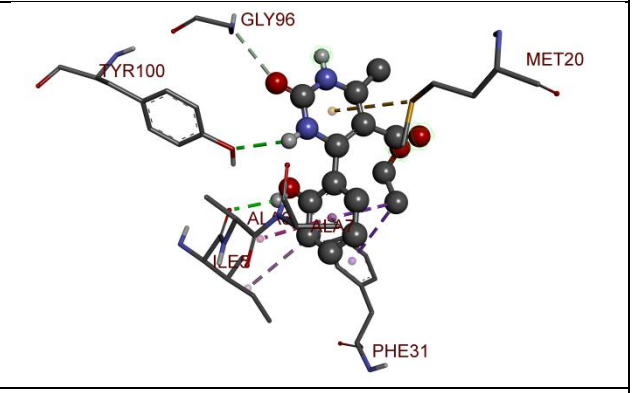
GLY96
TYR100
MET20
ILE5
PHE31

A6

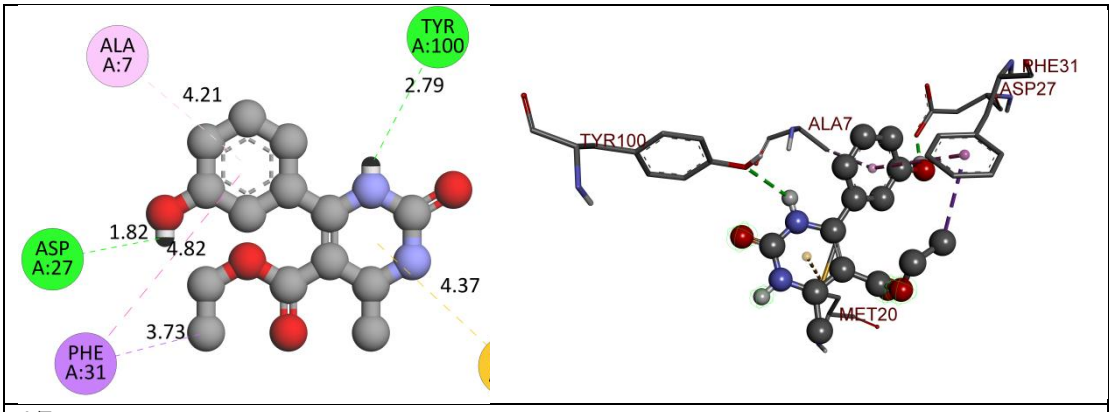

A7

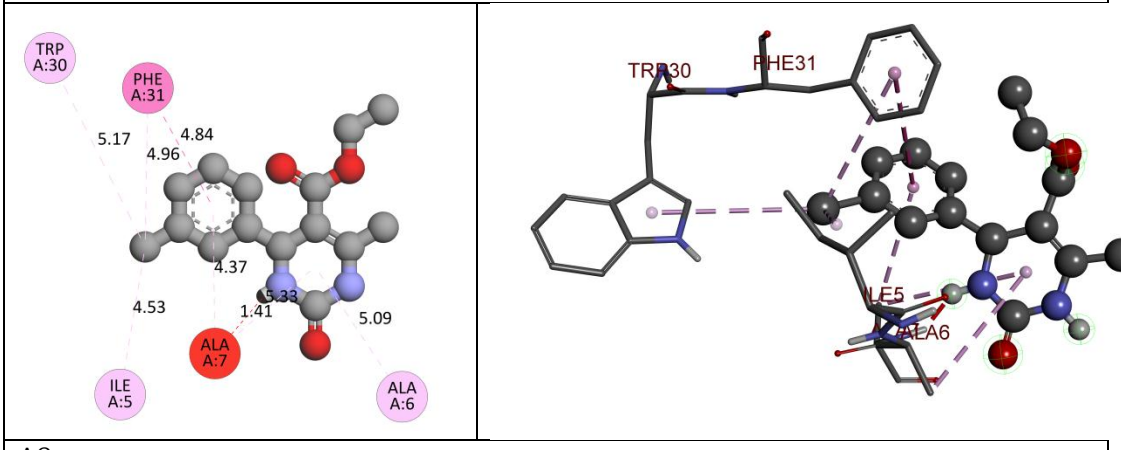

A8

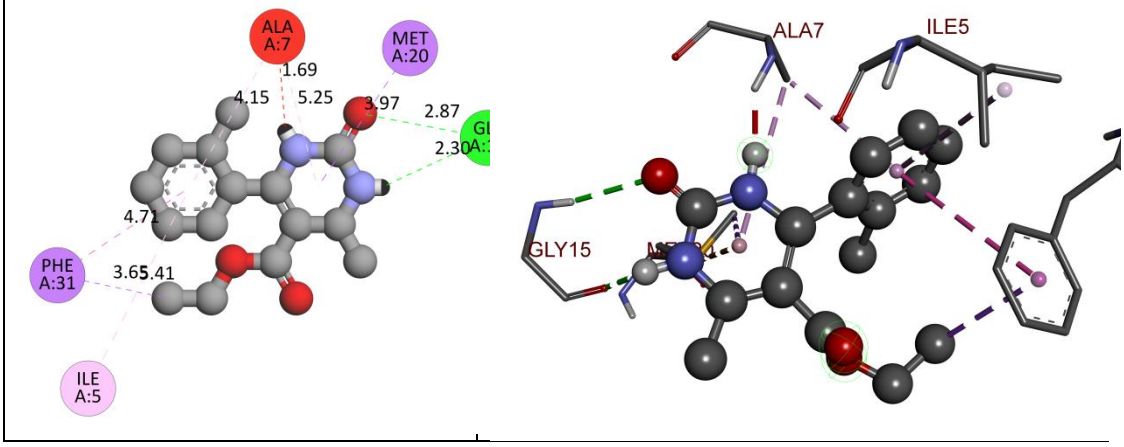

Table 9
The antimicrobial and antifungal activities of the synthesized derivatives

Compound code	Antimicrobial activity [*MIC* (μg/mL)]				Antifungal activity [*MFC* (μg/mL)]		
	E.C.	*P.A.*	*S.A.*	*S.P.*	*C.A.*	*A.N.*	*A.C.*

A1	125	50	225	125	150	150	150
A2	75	125	50	100	550	200	150
A3	50	25	50	150	550	150	150
A4	125	25	250	150	150	150	150
A5	125	50	50	150	150	150	150
A6	150	100	200	100	200	175	175
A7	50	100	100	125	100	150	200
A8	125	75	75	145	200	150	200
Gentamycin	0.05	1	0.25	0.5	NA	NA	NA
Ampicillin	100	NA	250	100	NA	NA	NA
Chloramphenicol	50	50	50	50	NA	NA	NA
Ciprofloxacin	25	25	50	50	NA	NA	NA
Norfloxacine	10	10	10	10	NA	NA	NA
Nystatin	NA	NA	NA	NA	100	100	100
Greseofulvin	NA	NA	NA	NA	500	100	100

Where: E.C., Escherichia coli; P.A., Pseudomonas aeruginosa; S.A., Staphylococcus aureus; S.P., Staphylococcus pyogenes; C.A., Candida albicans; A.N., Aspergillus niger; A.C., Aspergillus clavatus; MIC, Minimum inhibitory concentration; MFCs, minimum fungicidal concentration,NS,Non-sensitive

Discussion

In present study we have designed and developed some 1, 2, 3, 4-tetrahydropyrimidine derivatives as potential DHFR inhibitors. In accordance with Lipinski's and Veber's rule (Table 4), Native ligand has violated both the rules. The log P values of all the molecules were between the ranges -0.70 to 2.01 which indicates optimum lipophilicity. Lipophilicity is a significant feature of the molecule that affects how it works in the body(S. Khan et al., 2021). It is determined by the compound's Log P value, which measures the drug's permeability in the body to reach the target tissue(Krzywinski & Altman, 2013; Lipinski et al., 2012). The molecular weight of all the molecules was below 500 Da which indicates active better transport of the molecules through biological membrane. Fortunately, the Lipinski rule of 5 had not been compromised by the compounds, excluding native ligand which displayed 2 violations of Lipinski rule respectively(A. Khan et al., 2022; Shntaif et al., 2021). The total polar surface area (TPSA) and the number of rotatable bonds have been found to better discriminate between compounds that are orally active or not. According to Veber's rule, TPSA should be ≤ 140 and number of rotatable bonds should be ≤ 10. It was observed that native ligand violated the Veber's rule, as it has TPSA 187.50$Å^2$ and number of rotatable bonds 10 which indicate its poor oral bioavailability.

In order to further optimize the compounds, pharmacokinetics and drug-likeness properties were calculated for each one. All the compounds including native ligand showed no penetration to the blood-brain barrier (BBB). The log *Kp* (skin penetration, cm/s) and bioavailability values of all the compounds were within acceptable limits. Native ligand do not meet all, two, or one of the Ghose, Egan, and Muegge requirements also showed lower GI absorption (Table 5). In acute toxicity predictions, native ligand and A8 fall in toxicity class-III i.e. toxic if swallowed ($50<LD_{50}\leq300$). Molecules A3, A4 and A7 displayed toxicity class-IV

which means harmful if swallowed ($300<LD_{50}\leq2000$). Molecules A1, A2, A5 and A6 showed toxicity class-V which indicate may be harmful if swallowed ($2000<LD_{50}\leq5000$)(Banerjee et al., 2018). From this virtual screening, it was concluded that all the compounds possess drug-like properties and hence were subjected to molecular docking studies.

The binding affinities of the derivatives have been compared with the binding mode of native ligand present in the crystal structure of DHFR (PDB ID: 5CCC). Native ligand exhibited -8.6 kcal/mol binding affinity with DHFR and formed 6 conventional hydrogen bonds with Asp27, Ile5, Arg57 and one carbon-hydrogen bond with Ile94. It has developed many hydrophobic interactions such as Pi-cation, Pi-sigma, Pi-Pi T-shaped and Pi-alkyl bonds with Phe31, Ala7, Ile50, and Ile5. Compound A1 exhibited -7.6 kcal/mol binding affinity, formed one conventional hydrogen bond with Trp100 whereas developed Pi-sigma, Pi-sulfur hydrophobic interactions with Phe31 and Met20, Pi-Pi T-shaped & Pi-Alkyl hydrophobic bonds with Ile5 & Ala7. Compound A2 displayed -7.9 kcal/mol binding affinity, formed two conventional hydrogen bonds with Gly15 & Trp100 whereas it has developed one Pi-sigma Pi-sulfur hydrophobic bonds with Phe31 and Met20, Pi-Pi T-shaped & Pi-Alkyl hydrophobic bonds with & Ala7. Compounds A3 & A4 displayed -8.0 kcal/mol & -7.9 kcal/mol docking score and formed only one conventional hydrogen bond Tyr100 and two carbon-hydrogen bond with Gly95 and Gly96. It has developed Pi-alkyl hydrophobic interactions with Ala97, Trp 30 and Phe31 & Pi-Sigma type of hydrophobic Interactions with Phe31. Compounds A5, A6 & A8 showed -7.8, -7.7, -7.5 kcal/mol docking score, developed two conventional hydrogen bonds with Tyr100 and Ile5. Compound A8 has developed one Pi-alkyl type of hydrophobic interactions with Phe31, Met20 and Pi-sulfur, pi-pi T-shaped with PHE31, Ala7, Ile5 and Ala7.

Although the compounds were synthesized by three methods and the progression of reaction was monitored by TLC, we have investigated the most effective method suitable for the synthesis which can gave maximum yield and consumed complete starting material. We have subjected one compound for mass study to check which method can still have starting material peak in the crude obtained product. Compound A3 was selected to prove comparative effectiveness of the method in which p-chloro benzaldehyde was used as substituent. For the synthesis of compound A3, it took 107, 35, and 2 min to complete the reaction through conventional, ultrasonic, and microwave method respectively. It was also observed that yield of the compound was very good in microwave assisted synthesis i.e. 73.24% which is almost 30-40% more than that of the conventional and ultrasonic method. In mass spectrum it was observed that, product obtained through microwave method was completely pure and did not displayed any peak of starting material, whereas product obtained through conventional and ultrasonic method showed presence of starting material. It means even after taking much time for the reaction and consuming more energy starting material did not get consumed in these both methods which ultimately affected on their product yield. A detailed comparative mass analysis of compound is explained in Fig. 3.

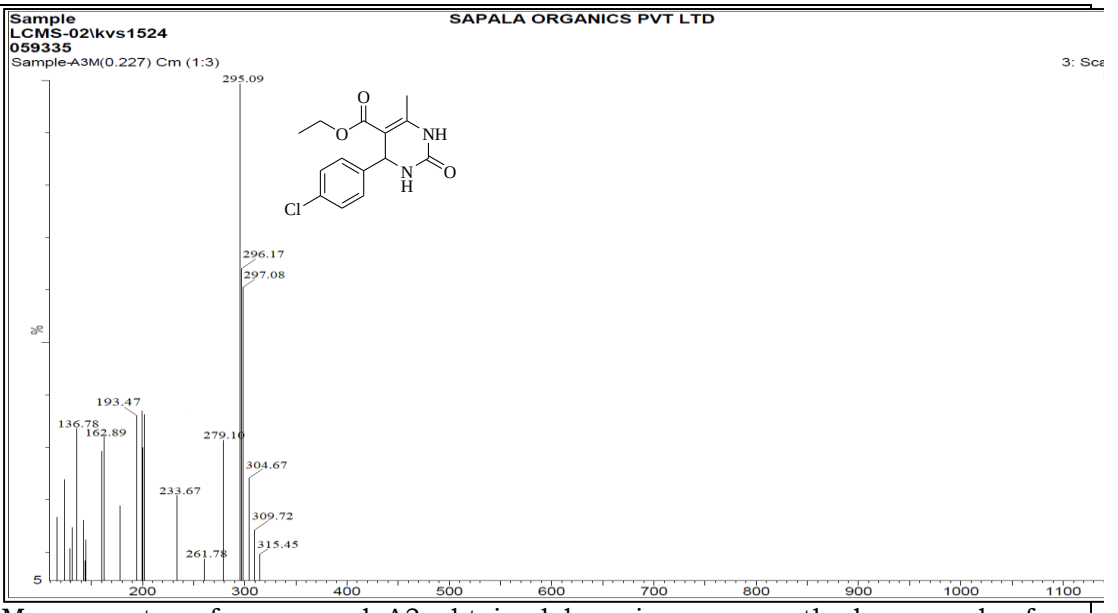

Mass spectra of compound A3 obtained by microwave method, no peak of p-chlorobenzaldehyde at 140 indicating complete consumption of it which gave higher yield of product.

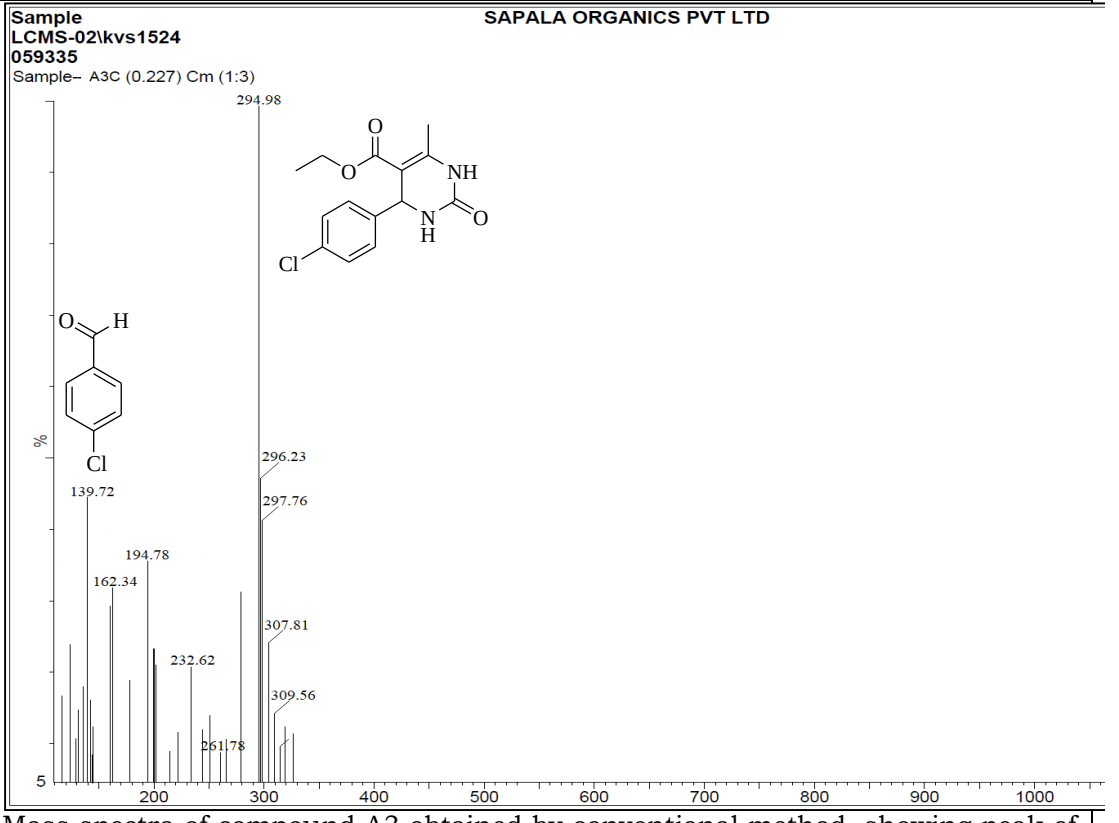

Mass spectra of compound A3 obtained by conventional method, showing peak of p-chlorobenzaldehyde at 139.72 indicating presence of starting material which

gave less yield of product.

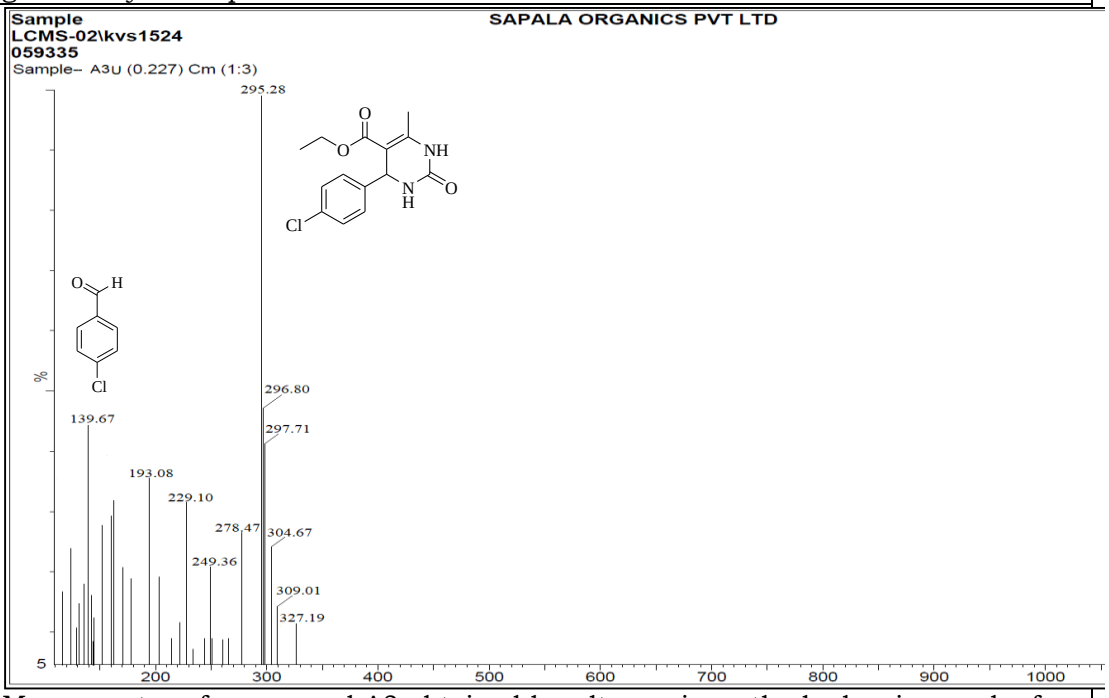

Mass spectra of compound A3 obtained by ultrasonic method, showing peak of p-chlorobenzaldehyde at 139.67 indicating presence of starting material which gave less yield of product.

Fig 3. Comparative mass spectrum analysis of compound A3 synthesized by conventional, ultrasonic and microwave method

Millions of humans are now affected by bacterial diseases triggered by pathogenic bacteria which are responsible for elevated child mortality rates in developed countries. Not all bacteria are pathogenic. For example, there are thousands of bacterial organisms in the human digestive tract, some of which are harmless and even useful. Furthermore, various mechanisms of action on the target site can aid in the discovery of potential drugs while developing antibacterial agents. However, since bacteria have developed antibiotic tolerance, finding a new antibacterial agent became difficult. Gram-positive bacteria, such as *methicillin-resistant S. aureus, S. epidermis, vancomycin-resistant E. calcium,* and *penicillin-resistant S. pneumoniae,* induce the majority of bacterial infections. Fungal infections have become more frequent, and the majority of them are minor. There are various varieties of fungi that cause infections today(S. Khan et al., 2021; Shntaif et al., 2021). Species like *candida* and *aspergillus* are only a few examples. In present investigation, all the synthesized compounds were subjected for *in vitro* antibacterial and antifungal activity using different strains as given in Table 9.

All the synthesized compounds were sensitive to gram +ve (*Staphylococcus aureus, Staphylococcus pyogenes*) and gram –ve (*Escherichia coli, Pseudomonas aeruginosa*) bacterial strains. All the compounds demonstrated more potent activity than Ampicillin against both gram-positive and gram-negative bacteria. All the compounds A1-A8 were sensitive against *Staphylococcus aureus* strains &

found to be more potent than the standard drug Ampicillin. Compounds A2, A3 & A7 were sensitive at 75, 50 &50 µg/mL against *Escherichia coli*. All the Compounds A1-A8 were sensitive at 50, 100, 200 & 250 µg/mL against *Staphylococcus aureus*. In antifungal activity, compound A7 was found to be more potent with MFCs 100 µg/mL against *Candida albicans*. It can be concluded that substitution at meta-position with bulky group can greatly increase the activity of the designed compounds.

Conclusion

Dihydrofolate reductase (DHFR) is an important enzyme required to maintain bacterial growth, and hence inhibitors of DHFR have been proven as effective agents for treating bacterial infections. In present study we have designed and developed some 1, 2, 3, 4-tetrahydropyrimidine derivatives as potential DHFR inhibitors. The designed derivatives were screened through Lipinski rule, Veber's rule, ADMET analysis, drug-likeness properties, and molecular docking. The selected derivatives were synthesized and subjected for *in vitro* biological evaluation. It was also observed that yield of the compound was very good in microwave assisted synthesis i.e. 73.24% which is almost 30-40% more than that of the conventional and ultrasonic method. In mass spectrum it was observed that, product obtained through microwave method was completely pure and did not displayed any peak of starting material, whereas product obtained through conventional and ultrasonic method showed presence of starting material. Therefore we concluded that the microwave assisted synthesis method is most suitable for the synthesis of tetrahydropyrimidine derivatives through Biginelli reaction. We hereby report that, all the compounds A1, A2, A3, A4, A5, A6, A7, and A8 were found to be are potent and can be developed further to get more promising molecules for the treatment of bacterial & fungal infections.

References

Ahmed Elkanzi, N. A. (2020). Synthesis and Biological Activities of Some Pyrimidine Derivatives: A Review. *Oriental Journal Of Chemistry*, *36*(6), 1001–1015. https://doi.org/10.13005/ojc/360602

Anwar, K., Hussein, D., & Salih, J. (2020). Antimicrobial susceptibility testing and phenotypic detection of MRSA isolated from diabetic foot infection. *International Journal of General Medicine*, *13*, 1349–1357. https://doi.org/10.2147/IJGM.S278574

Banerjee, P., Eckert, A. O., Schrey, A. K., & Preissner, R. (2018). ProTox-II: A webserver for the prediction of toxicity of chemicals. *Nucleic Acids Research*, *46*(W1), W257–W263. https://doi.org/10.1093/nar/gky318

Bhat, A. R., Dongre, R. S., Naikoo, G. A., Hassan, I. U., & Ara, T. (2017). Proficient synthesis of bioactive annulated pyrimidine derivatives: A review. *Journal of Taibah University for Science*, *11*(6), 1047–1069. https://doi.org/10.1016/j.jtusci.2017.05.005

Chaudhari, R. N., Khan, S. L., Chaudhary, R. S., Jain, S. P., & Siddiqui, F. A. (2020). B-Sitosterol: Isolation from Muntingia Calabura Linn Bark Extract, Structural Elucidation And Molecular Docking Studies As Potential Inhibitor of SARS-CoV-2 Mpro (COVID-19). *Asian Journal of Pharmaceutical and Clinical Research*, *13*(5), 204–209. https://doi.org/10.22159/ajpcr.2020.v13i5.37909

Daina, A., Michielin, O., & Zoete, V. (2017). SwissADME: A free web tool to evaluate pharmacokinetics, drug-likeness and medicinal chemistry friendliness of small molecules. *Scientific Reports*, *7*. https://doi.org/10.1038/srep42717

Dallakyan, S., & Olson, A. J. (2015). Small-molecule library screening by docking with PyRx. *Methods in Molecular Biology*, *1263*(1263), 243–250. https://doi.org/10.1007/978-1-4939-2269-7_19

Jouhar, L., Jaafar, R. F., Nasreddine, R., Itani, O., Haddad, F., Rizk, N., & Hoballah, J. J. (2020). Microbiological profile and antimicrobial resistance among diabetic foot infections in Lebanon. *International Wound Journal*, *17*(6), 1764–1773. https://doi.org/10.1111/iwj.13465

Khan, A., Unnisa, A., Sohel, M., Date, M., Panpaliya, N., Saboo, S. G., Siddiqui, F., & Khan, S. (2022). Investigation of phytoconstituents of Enicostemma littorale as potential glucokinase activators through molecular docking for the treatment of type 2 diabetes mellitus. *In Silico Pharmacology*, *10*(1). https://doi.org/10.1007/s40203-021-00116-8

Khan, S., Kale, M., Siddiqui, F., & Nema, N. (2021). Novel pyrimidine-benzimidazole hybrids with antibacterial and antifungal properties and potential inhibition of SARS-CoV-2 main protease and spike glycoprotein. *Digital Chinese Medicine*, *4*(2), 102–119. https://doi.org/10.1016/j.dcmed.2021.06.004

Khan, S.L., Siddiqui, F. A., Jain, S. P., & Sonwane, G. M. (2020). Discovery of Potential Inhibitors of SARS-CoV-2 (COVID-19) Main Protease (Mpro) from Nigella Sativa (Black Seed) by Molecular Docking Study. *Coronaviruses*, *2*(3), 384–402. https://doi.org/10.2174/2666796701999200921094103

Khan, Sharuk L., Siddiqui, F. A., Shaikh, M. S., Nema, N. V., & Shaikh, A. A. (2021). Discovery of potential inhibitors of the receptor-binding domain (RBD) of pandemic disease-causing SARS-CoV-2 Spike Glycoprotein from Triphala through molecular docking. *Current Chinese Chemistry*, *01*. https://doi.org/10.2174/2666001601666210322121802

Khan, Sharuk L., Sonwane, G. M., Siddiqui, F. A., Jain, S. P., Kale, M. A., & Borkar, V. S. (2020). Discovery of Naturally Occurring Flavonoids as Human Cytochrome P450 (CYP3A4) Inhibitors with the Aid of Computational Chemistry. *Indo Global Journal of Pharmaceutical Sciences*, *10*(04), 58–69. https://doi.org/10.35652/igjps.2020.10409

Kim, S., Chen, J., Cheng, T., Gindulyte, A., He, J., He, S., Li, Q., Shoemaker, B. A., Thiessen, P. A., Yu, B., Zaslavsky, L., Zhang, J., & Bolton, E. E. (2021). PubChem in 2021: New data content and improved web interfaces. *Nucleic Acids Research*, *49*(D1), D1388–D1395. https://doi.org/10.1093/nar/gkaa971

Krzywinski, M., & Altman, N. (2013). Points of significance: Significance, P values and t-tests. *Nature Methods*, *10*(11), 1041–1042. https://doi.org/10.1038/nmeth.2698

Lipinski, C. A., Lombardo, F., Dominy, B. W., & Feeney, P. J. (2012). Experimental and computational approaches to estimate solubility and permeability in drug discovery and development settings. In *Advanced Drug Delivery Reviews* (Vol. 64, Issue SUPPL., pp. 4–17). https://doi.org/10.1016/j.addr.2012.09.019

Loi, V. Van, Huyen, N. T. T., Busche, T., Tung, Q. N., Gruhlke, M. C. H., Kalinowski, J., Bernhardt, J., Slusarenko, A. J., & Antelmann, H. (2019). Staphylococcus aureus responds to allicin by global S-thioallylation – Role of the Brx/BSH/YpdA pathway and the disulfide reductase MerA to overcome

allicin stress. *Free Radical Biology and Medicine*, *139*, 55–69. https://doi.org/10.1016/j.freeradbiomed.2019.05.018

Mittersteiner, M., Farias, F. F. S., Bonacorso, H. G., Martins, M. A. P., & Zanatta, N. (2021). Ultrasound-assisted synthesis of pyrimidines and their fused derivatives: A review. *Ultrasonics Sonochemistry*, *79*. https://doi.org/10.1016/j.ultsonch.2021.105683

Murali, T. S., Kavitha, S., Spoorthi, J., Bhat, D. V., Prasad, A. S. B., Upton, Z., Ramachandra, L., Acharya, R. V., & Satyamoorthy, K. (2014). Characteristics of microbial drug resistance and its correlates in chronic diabetic foot ulcer infections. *Journal of Medical Microbiology*, *63*, 1377–1385. https://doi.org/10.1099/jmm.0.076034-0

Nepali, K., Sharma, S., Sharma, M., Bedi, P. M. S., & Dhar, K. L. (2014). Rational approaches, design strategies, structure activity relationship and mechanistic insights for anticancer hybrids. *European Journal of Medicinal Chemistry*, *77*, 422–487. https://doi.org/10.1016/j.ejmech.2014.03.018

Nerkar, A. U. (2021). Use of Pyrimidine and Its Derivative in Pharmaceuticals: A Review. *Journal of Advanced Chemical Sciences*, *7*(2), 729–732. https://doi.org/10.30799/jacs.239.21070203

Rappé, A. K., Casewit, C. J., Colwell, K. S., Goddard, W. A., & Skiff, W. M. (1992). UFF, a Full Periodic Table Force Field for Molecular Mechanics and Molecular Dynamics Simulations. *Journal of the American Chemical Society*, *114*(25), 10024–10035. https://doi.org/10.1021/ja00051a040

San Diego: Accelrys Software Inc. (2012). Discovery Studio Modeling Environment, Release 3.5. *Accelrys Software Inc.* https://www.3dsbiovia.com/about/citations-references/

Sánchez-Sánchez, M., Cruz-Pulido, W. L., Bladinieres-Cámara, E., Alcalá-Durán, R., Rivera-Sánchez, G., & Bocanegra-García, V. (2017). Bacterial Prevalence and Antibiotic Resistance in Clinical Isolates of Diabetic Foot Ulcers in the Northeast of Tamaulipas, Mexico. *International Journal of Lower Extremity Wounds*, *16*(2), 129–134. https://doi.org/10.1177/1534734617705254

Shahi, S. K., & Kumar, A. (2016). Isolation and genetic analysis of multidrug resistant bacteria from diabetic foot ulcers. *Frontiers in Microbiology*, *6*(JAN). https://doi.org/10.3389/fmicb.2015.01464

Shen, Z. L., Xu, X. P., & Ji, S. J. (2010). Brønsted base-catalyzed one-pot three-component Biginelli-type reaction: An efficient synthesis of 4,5,6-triaryl-3,4-dihydropyrimidin-2(1H)-one and mechanistic study. *Journal of Organic Chemistry*, *75*(4), 1162–1167. https://doi.org/10.1021/jo902394y

Shntaif, A. H., Khan, S., Tapadiya, G., Chettupalli, A., Saboo, S., Shaikh, M. S., Siddiqui, F., & Amara, R. R. (2021). Rational drug design, synthesis, and biological evaluation of novel N-(2-arylaminophenyl)-2,3-diphenylquinoxaline-6-sulfonamides as potential antimalarial, antifungal, and antibacterial agents. *Digital Chinese Medicine*, *4*(4), 290–304. https://doi.org/10.1016/j.dcmed.2021.12.004

Siddiqui, F. A., Khan, S. L., Marathe, R. P., & Nema, N. V. (2021). Design, Synthesis, and In Silico Studies of Novel N-(2-Aminophenyl)-2,3-Diphenylquinoxaline-6-Sulfonamide Derivatives Targeting Receptor- Binding Domain (RBD) of SARS-CoV-2 Spike Glycoprotein and their Evaluation as Antimicrobial and Antimalarial Agents. *Letters in Drug Design & Discovery*, *18*(9), 915–931. https://doi.org/10.2174/1570180818666210427095203

Todd, M. J., & Gomez, J. (2001). Enzyme kinetics determined using calorimetry: A

general assay for enzyme activity? *Analytical Biochemistry*, *296*(2), 179–187. https://doi.org/10.1006/abio.2001.5218

Verma, V., Joshi, C. P., Agarwal, A., Soni, S., & Kataria, U. (2020). A Review on Pharmacological Aspects of Pyrimidine Derivatives. *Journal of Drug Delivery and Therapeutics*, *10*(5), 358–361. https://doi.org/10.22270/jddt.v10i5.4295

Wróbel, A., Arciszewska, K., Maliszewski, D., & Drozdowska, D. (2020). Trimethoprim and other nonclassical antifolates an excellent template for searching modifications of dihydrofolate reductase enzyme inhibitors. *Journal of Antibiotics*, *73*(1), 5–27. https://doi.org/10.1038/s41429-019-0240-6